

p-wave Pairing in a Two-Component Fermi System with Unequal Population: Weak Coupling BCS to Strong Coupling BEC Regimes

Renyuan Liao, Florentin Popescu, and Khandker Quader
Department of Physics, Kent State University, Kent, OH 44242
 (Dated: August 17, 2021)

We study p -wave pairing in a two-component Fermi system with unequal population across weak-coupling BCS to strong-coupling BEC regimes. We find a rich $m_s = 0$ spin triplet p -wave superfluid (SF) ground state (GS) structure as a function of population imbalance. Under a phase stability condition, the “global” energy minimum is given by a multitude of “mixed” SF states formed of linear combinations of $m = \pm 1, 0$ sub-states of the $\ell = 1$ orbital angular momentum state. Except for the “pure” SF states, ($\ell = 1, m = \pm 1$), other states exhibit oscillation in energy with the relative phase between the constituent gap amplitudes. We also find states with “local” energy minimum that can be stable at higher polarizations, suggesting a quantum phase transition between the “global” and “local” minima phases driven by polarization. We relate the local and global minimum states to Morse and non-Morse critical points. We calculate the variations of the ground state energy with a relative phase angle, coupling and polarization, and discuss possible consequences for experiments.

PACS numbers: 03.75.Ss, 05.30.Fk, 74.20.Rp, 74.20.De, 67.85.-d, 67.85.Fg, 34.50.-s

I. INTRODUCTION

Over past several years there has been sustained experimental and theoretical interest in paired fermion ground states with unconventional pairing symmetry. Among these are various types of p -wave spin triplet condensates. Correlated electron systems, such as, SrRu_2O_4 ¹ and ferromagnetic superconductors² are believed to possess p -wave triplet symmetry. Fermi systems with unequal species population, as in quark matter³, magnetic field induced organic superconductors⁴ and in cold fermion systems with unequally populated hyperfine states⁵, add a fascinating dimension. Discovery of s -wave superfluidity in cold atoms⁶ subjected to s -wave Feshbach resonance (FR), and observations of p -wave FR^{7–10} in ${}^6\text{Li}$ and ${}^{40}\text{K}$ had raised the prospect for observing p -wave superfluidity in cold fermi gases. While this may not be as easy, alternate methods¹¹ and optical lattices^{12,13} offer encouraging prospects. Past theory work on p -wave superfluidity in the BEC-BCS crossover region include those for a single-component Fermi gas^{14–17}, as well as for the two-component case¹⁸ with equal-species population. However, theory work on p -wave pairing for unequal species population has been limited^{13,19}.

In this paper, we study p -wave superfluidity in a two-component Fermi system with *unequal* population, across weak-coupling BCS to strong coupling BEC regimes. We focus on the case where inter-species pairing interaction is dominant. While this is interesting to study on general grounds, we are also motivated by work¹³ on population imbalanced Fermi mixtures in optical lattices, and by the observation^{9,18} that unlike liquid ${}^3\text{He}$, pairing interaction in cold atoms may be highly anisotropic in “spin”-space. (“spin” referring to hyperfine states). For example, in ${}^6\text{Li}$, when the hyperfine pair $|m_s, m'_s\rangle = |1/2, -1/2\rangle$ is at resonance, the pairs $|1/2, 1/2\rangle$ and $|-1/2, -1/2\rangle$ would not be. So, intra-spin interactions can be neglected. Pairs in p -wave superfluids with unlike “spin”

components can, however, have different $\ell = 1$ components, namely, $m = \pm 1, 0$; the gap parameters $\Delta_{\ell=1,m}$ are related to the spherical harmonics, $Y_{1,m=\pm 1,0}$.

Our study of the population imbalanced Fermi system lead to several new results and predictions. These should appeal broadly to systems exhibiting p -wave pairing, especially those with population imbalance between species. We find a rich superfluid (SF) ground state (GS) structure. Under a condition on relative phase between three pairing amplitudes Δ_m 's ($\Delta_{\ell=1,m} \equiv \Delta_m$ hereforth), a multitude of “mixed” superfluid states of the form $a_0\Delta_0 + a_1\Delta_1 + a_{-1}\Delta_{-1}$ are found to be degenerate with $\Delta_{\pm 1}$; these give the *global* minimum GS energy. In addition, we find states with *local* minimum energy. We provide a geometric representation of the p -wave SF states (Fig. 1). Our zero temperature polarization (P) vs p -wave coupling phase diagram (Fig. 2) shows two superfluid phases, comprising of states with global and local minimum energy respectively, and a region of phase separation. Our results suggest the possibility of a quantum phase transition between the two superfluid phases, driven by polarization. We find the $P \neq 0$ ground state structure to be preserved in the $P \rightarrow 0$ limit; hence richer than that obtained earlier¹⁸ for $P = 0$. The energies of the “mixed” states show oscillations with the relative phase angle (Fig.3), that may be interesting to explore experimentally. We also study the behavior of superfluid ground state energy with coupling and polarization.

The paper is organized as follows. In Sec. II, we present the model used for describing the two-component Fermi system with unequal spin population across the BCS to BEC regimes. We provide details of the finite-temperature imaginary-time Green's function method used for obtaining the coupled p -wave gap and number equations, and the grand canonical potential. In Sec. III, we carry out a free energy analysis of the p -wave ground states in a population imbalanced system. We provide

details of the derivation of the free energy to quartic order in pairing gap amplitudes, and the expansion coefficients in terms of the underlying coupling and polarization. This section also shows how minimization of the free energy leads to conditions of stability of p-wave superfluid phases and the nature of the states that may give rise to global and local minima of the free energy. A geometric depiction is provided for a clearer understanding of the possible p-wave states, and the dependence of some of the states on a phase angle. To provide a perspective on the stability of the states, we also present here a brief discussion of connection of the stable states to "critical points" in Catastrophe Theory. In Sec. IV, we discuss our self-consistent solutions of coupled gap and number equations for fixed polarization and coupling parameter. We outline how the free energy expansion coefficients and the free energy are obtained, and the scheme by which the p-wave coupling vs polarization phase diagram across BEC-BCS regimes is constructed (Sec IVA). Our study of the variation of the free-energy with phase angle, coupling and polarization is discussed in Sec IVB. We conclude with a summary of the work and discussions in Sec. V.

II. MODEL AND DEVELOPMENT

We consider a Fermi system with unequal "spin" ($(\uparrow, \downarrow) \equiv (1/2, -1/2)$) population, and with all fermions having the same mass. Pairing interactions in all three $\ell = 1$ channels ($m = 0, \pm 1$) are taken to be equal, and intra-species interactions ($\uparrow\uparrow$ or $\downarrow\downarrow$) are set to zero. Since we adjust self-consistently the chemical potential with the strength and sign of the coupling, in our fermion-only model, molecules would appear naturally as 2-fermion bound states. The $S = 1, m_s = 0$ triplet pairing Hamiltonian is then given by:

$$\mathcal{H} = \sum_{\mathbf{k}\sigma} \xi_{\mathbf{k}\sigma} c_{\mathbf{k}\sigma}^\dagger c_{\mathbf{k}\sigma} + \sum_{\mathbf{k}\mathbf{k}'\mathbf{q}} V_{\mathbf{k}\mathbf{k}'} c_{\mathbf{k}+\mathbf{q}/2\uparrow}^\dagger c_{-\mathbf{k}+\mathbf{q}/2\downarrow}^\dagger c_{-\mathbf{k}'+\mathbf{q}/2\downarrow} c_{\mathbf{k}'+\mathbf{q}/2\uparrow} \quad (1)$$

where $c_{\mathbf{k}\sigma}$ ($c_{\mathbf{k}\sigma}^\dagger$) is the annihilation (creation) operator for a fermion with momentum \mathbf{k} , kinetic energy $\xi_{\mathbf{k}\sigma} = \epsilon_{\mathbf{k}} - \mu_\sigma$, and spin σ ; μ_σ is the chemical potential of each component, and $\epsilon_{\mathbf{k}} = \hbar^2 k^2 / 2m$. $V_{\mathbf{k}\mathbf{k}'}$ is the pairing interaction.

We consider condensate pairs with zero center-of-mass momentum, ($\mathbf{q}=0$). While non-zero \mathbf{q} would be interesting from the perspective of FFLO²⁰ states, the problem of $\mathbf{q} = 0$ unconventional pairing in systems with unequal population is rich in itself. \mathcal{H} is mean-field (MF) decoupled via the $S = 1, m_s = 0$ "spin"-triplet pairing gap

function $\Delta_{\downarrow\uparrow}(\mathbf{k}) \equiv \Delta(\mathbf{k}) = -\sum_{\mathbf{k}'} V_{\mathbf{k}\mathbf{k}'} \langle c_{-\mathbf{k}'\downarrow} c_{\mathbf{k}'\uparrow} \rangle$ giving:

$$\mathcal{H}^{\text{MF}} = \sum_{\mathbf{k}\sigma} \xi_{\mathbf{k}\sigma} c_{\mathbf{k}\sigma}^\dagger c_{\mathbf{k}\sigma} - \sum_{\mathbf{k}} \left[\Delta(\mathbf{k}) c_{\mathbf{k}\uparrow}^\dagger c_{-\mathbf{k}\downarrow}^\dagger + \text{H.c.} \right] - \sum_{\mathbf{k}, \mathbf{k}'} V_{\mathbf{k}\mathbf{k}'} \langle c_{\mathbf{k}\uparrow}^\dagger c_{-\mathbf{k}\downarrow}^\dagger \rangle \langle c_{-\mathbf{k}'\downarrow} c_{\mathbf{k}'\uparrow} \rangle \quad (2)$$

To obtain the ground state energy of the mean-field Hamiltonian (2) we use the equation-of-motion method^{22,23} for the imaginary-time ($\tau = it$) normal ($G_{\sigma\sigma'}$) and anomalous ($F_{\sigma\sigma'}$) Green's functions, defined in the usual way as²² as time-ordered expectation values of the fermion creation and annihilation operators: $G_{\sigma,\sigma'} \equiv -\langle T_\tau c_{\mathbf{k}\sigma}(\tau) c_{\mathbf{k}\sigma'}^\dagger(0) \rangle$, and $F_{\sigma,\sigma'} \equiv -\langle T_\tau c_{-\mathbf{k}\sigma}^\dagger(\tau) c_{\mathbf{k}\sigma'}^\dagger(0) \rangle$. The equations of motions that follow from these are given by:

$$\partial_\tau G_{\sigma\sigma'}(\mathbf{k}, \tau) = -\delta(\tau) \delta_{\sigma\sigma'} - \xi_{\mathbf{k}\sigma} G_{\sigma\sigma'}(\mathbf{k}, \tau) + \Delta_{-\sigma\sigma}(\mathbf{k}) F_{-\sigma\sigma'}(\mathbf{k}, \tau), \quad (3)$$

$$\partial_\tau F_{\sigma\sigma'}(\mathbf{k}, \tau) = \xi_{-\mathbf{k}\sigma} F_{\sigma\sigma'}(\mathbf{k}, \tau) + \Delta_{\sigma-\sigma}^*(\mathbf{k}) G_{-\sigma\sigma'}(\mathbf{k}, \tau). \quad (4)$$

Eqs.(3) and (4) are Fourier transformed with $\tau \rightarrow i\omega_n \equiv \nu$ and $\partial_\tau \rightarrow -\nu$, where $i\omega_n = (2n+1)\pi T$ are Matsubara frequencies. This gives:

$$G_{\sigma\sigma}(\mathbf{k}, \nu) = \frac{-\xi_{-\mathbf{k}-\sigma} + \nu}{(\xi_{\mathbf{k}\sigma} - \nu)(\xi_{-\mathbf{k}-\sigma} + \nu) + |\Delta_{\sigma,-\sigma}(\mathbf{k})|^2} \quad (5)$$

$$F_{\sigma-\sigma}(\mathbf{k}, \nu) = \frac{\Delta_{\sigma-\sigma}^*(\mathbf{k})}{(\xi_{\mathbf{k}-\sigma} - \nu)(\xi_{-\mathbf{k}\sigma} + \nu) + |\Delta_{\sigma-\sigma}(\mathbf{k})|^2} = -F_{-\sigma\sigma}(\mathbf{k}, \nu) \quad (6)$$

In terms of radial and angular parts, the pairing interaction can be written in the form:

$$V_{\mathbf{k}\mathbf{k}'} = (4\pi/3) \sum_m V_{kk'} Y_{1,m}(\hat{\mathbf{k}}) Y_{1,m}^*(\hat{\mathbf{k}}'), \quad (7)$$

with $\hat{\mathbf{k}} = (\theta, \phi)$. Using $\langle c_{-\mathbf{k}'\downarrow} c_{\mathbf{k}'\uparrow} \rangle \equiv F_{\downarrow\uparrow}^*(\mathbf{k}', \tau=0^-)$ and Eq.(6), we obtain, $\Delta(\mathbf{k}) = -(1/k_B T) \sum_{\nu\mathbf{k}'} V_{\mathbf{k}\mathbf{k}'} F_{\downarrow\uparrow}^*(\mathbf{k}', \nu) e^{\nu 0^+}$. We take $V_{kk'} = \lambda w(k) w(k')$, a separable form chosen for convenience;^{16,18,24} this does not qualitatively change the physics. This gives for the gap function: $\Delta(\mathbf{k}) = \sum_m \Delta_m w(k) Y_{1,m}(\hat{\mathbf{k}}) \equiv w(k) \Delta(\hat{\mathbf{k}})$, where $\Delta_m = -(1/k_B T) \sum_{\nu\mathbf{k}'} \lambda w(k') Y_{1,m}^*(\hat{\mathbf{k}}') F_{\downarrow\uparrow}^*(k', \nu) e^{\nu 0^+}$. Using the Fourier transform $F_{\downarrow\uparrow}(k, \nu)$ from Eq.(6), and the definition of $G_{\sigma\sigma}$ above, we deduce equations for the $\ell = 1; m = 0, \pm 1$ gap amplitudes,

$$\Delta_m = -\lambda \sum_{\mathbf{k}} w(k) Y_{1,m}^*(\hat{\mathbf{k}}) \Delta(\mathbf{k}) [n_F(E_k^-) - n_F(E_k^+)] / (2E_k) \quad (8)$$

and for the particle number densities,

$$n_\sigma = \sum_{\mathbf{k}} \langle c_{\mathbf{k}\sigma}^\dagger c_{\mathbf{k}\sigma} \rangle = \sum_{\mathbf{k}} G_{\sigma\sigma}(k, \tau = 0^-). \quad (9)$$

Above, $E_k = [\xi_k^2 + |\Delta^2(\mathbf{k})|]^{1/2}$, with $\xi_k = (\xi_{k\uparrow} + \xi_{k\downarrow})/2 = \epsilon_k - \mu$ and $\mu = (\mu_\uparrow + \mu_\downarrow)/2$; $n_F(E_k^\pm)$ are Fermi functions, with $E_k^\pm = -h \pm E_k$, where $h = (\xi_{k\downarrow} - \xi_{k\uparrow})/2 = (\mu_\uparrow - \mu_\downarrow)/2$. At $T=0$ and for $h>0$, the expectation value of the grand canonical potential is given by:

$$E_g \equiv \langle \mathcal{H} \rangle = \sum_k \left\{ \xi_k - E_k + \frac{|\Delta(\mathbf{k})|^2}{2\epsilon_k} \right\} + \sum_k \{ (E_k - h)\theta(-E_k + h) \} - \frac{1}{g} \sum_m |\Delta_m|^2 \quad (10)$$

Following standard practice, the coupling λ has been expressed in terms of the ‘‘regularized’’ interaction g : $1/g = 1/\lambda + (1/(2\pi\hbar)^3) \int w^2(k) d^3\mathbf{k}/2\epsilon_k$ ²⁵. For $w(k)$, we adopt the N-SR form²⁴: $w(k) = k_0 k / (k_0^2 + k^2)$.

III. FREE ENERGY ANALYSIS OF GROUND STATE

A. Free Energy to Quartic Order

First, we carry out an *analytic study* of the p-wave superfluid ground state structure by constructing a free energy to quartic order. We assume that $0 \leq |\Delta(\mathbf{k})| \ll \xi_k$, and expand E_k in Eq.(10) in powers of $|\Delta(\mathbf{k})|$ keeping terms to 4th order: $E_k \sim |\xi_k| [1 + |\Delta(\mathbf{k})|^2/2|\xi_k|^2 - |\Delta(\mathbf{k})|^4/8|\xi_k|^4]$. Note that since $\xi_k \gg |\Delta(\mathbf{k})|$, $\xi_k = 0$ ($\epsilon_k = \mu$) is excluded from the expansion. The reasoning is similar to that in Ref. 11, and can be seen on noting the following: $\sum_{E_k > h} E_k = \sum_{|\Delta_k| < |\xi_k|} \sqrt{|\Delta_k|^2 + \xi_k^2} = \sum_{|\Delta_k| < |\xi_k|} \sqrt{|\Delta_k|^2 + |\xi_k|^2} + \sum_{|\Delta_k| < |\xi_k|} \sqrt{|\Delta_k|^2 + \xi_k^2} = \sum_{|\Delta_k| < |\xi_k|, |\xi_k| > h} |O(\Delta_k)| + \sum_{|\Delta_k| < |\xi_k|, \xi_k > h} \sqrt{|\Delta_k|^2 + \xi_k^2}$. Owing to negligible integration domain, and small integrand, the first term is negligible compared to the second, giving $\sum_{E_k > h} E_k \simeq \sum_{|\Delta_k| < |\xi_k|, \xi_k > h} \sqrt{|\Delta_k|^2 + \xi_k^2}$; $\xi_k = 0$ is thus excluded. Substituting this in Eq.(10) and converting momentum sums to integrals we obtain:

$$E_g = \alpha \int |\Delta(\hat{k})|^2 d\Omega + \beta \int |\Delta(\hat{k})|^4 d\Omega + \gamma, \quad (11)$$

where

$$\begin{aligned} \alpha &= (1/(2\pi\hbar)^3) \int_{E_k < h} w^2(k) k^2 dk / 2\epsilon_k \\ &+ (1/(2\pi\hbar)^3) \int_{E_k > h} w^2(k) k^2 dk (1/2\epsilon_k - 1/2|\xi_k|) - 1/g \\ \beta &= (1/(2\pi\hbar)^3) \int_{E_k > h} w^4(k) k^2 dk / 8|\xi_k|^3 \\ \gamma &= (4\pi/(2\pi\hbar)^3) \int_{E_k < h} (\xi_k - h) k^2 dk. \end{aligned} \quad (12)$$

Existence of a superfluid phase requires $\alpha < 0$, otherwise minimization of E_g forces the gap to vanish. The polarization ($P = (n_\uparrow - n_\downarrow)/(n_\uparrow + n_\downarrow)$) dependence of E_g is contained in α, β, γ , which depend on h, μ and $w(k)$; α alone depends explicitly on the coupling g . Accordingly, the Δ_m 's are sensitive to changes in P .

For fixed μ, h , and keeping E_k to $\mathcal{O}(\Delta(\mathbf{k})^4)$, we obtain an analytic expression for the ground state energy, E_G , in terms of the pairing amplitudes Δ_m :

$$E_G = -\frac{\alpha^2}{8\beta} + \gamma + 2\beta \left(|\Delta_0|^2 + |\Delta_1|^2 + |\Delta_{-1}|^2 + \frac{\alpha}{4\beta} \right)^2 + \beta (|\Delta_0|^2 - 2|\Delta_1||\Delta_{-1}|)^2 + 4\beta(1-t)|\Delta_0|^2|\Delta_1||\Delta_{-1}| \quad (13)$$

where $t = \cos\theta$, with $\theta = \langle (\Delta_0\Delta_1^*, \Delta_0^*\Delta_{-1}) \rangle = 2\phi_0 - \phi_1 - \phi_{-1}$; ϕ_m 's are the phases associated with the gap amplitudes Δ_m .

B. Energy Minimization: Global and Local Minima

Minimizing E_G in (13) with respect to Δ_m 's, we find that for a stable p-wave superfluid phase to exist, the following conditions have to be satisfied simultaneously

$$\begin{aligned} (a) \quad & |\Delta_0|^2 + |\Delta_1|^2 + |\Delta_{-1}|^2 = -\alpha/4\beta \equiv R^2 \quad (\text{sphere}) \\ (b) \quad & |\Delta_0|^2 - 2|\Delta_1||\Delta_{-1}| = 0 \quad (\text{plane}) \\ (c) \quad & (1-t)|\Delta_0|^2|\Delta_1||\Delta_{-1}| = 0 \end{aligned} \quad (14)$$

For all three Δ_m 's non-zero, conditions 14(a) and 14(b) give a semicircle formed by the intersection of the surface of a sphere of radius R , ($R^2 = -\alpha/4\beta$), in the space of $\Delta_1, \Delta_{-1}, \Delta_0$, with a plane defined by $|\Delta_1| + |\Delta_{-1}| = R$. The points spanning the semicircle represent a multitude of ‘‘mixed’’ superfluid states of the form $a_0\Delta_0 + a_1\Delta_1 + a_{-1}\Delta_{-1}$; a_0, a_1, a_{-1} being constants. A 3D geometric representation of the states is shown in Fig.1. The third condition 14(c) imposes the constraint, $t \equiv \cos\theta = 1$, i.e. the relative phase $\theta = (\phi_0 - \phi_1) - (\phi_{-1} - \phi_0) = 2n\pi$. $t=1$ corresponds to a parallel orientation of vectors $\Delta_0\Delta_1^*$ and $\Delta_0^*\Delta_{-1}$. The calculated ground state (GS) *global minimum* energy,

$$E_G^{gl} = -\alpha^2/8\beta + \gamma, \quad (\alpha < 0), \quad (15)$$

is completely determined by α, β , and γ given earlier.

The phase condition 14(c) is always satisfied for the states, $\Delta_{\pm 1}$, at the endpoints A and B of the semicircle. But, the energies of the states on the semicircle, other than A, B, oscillate with θ , and attains the global minimum E_G^{gl} only for $t = 1$, i.e. $\theta = 2n\pi$ (Fig. 3a). The oscillation amplitude depends on the specific state; e.g. state C at the top of the projected figure (Fig.1) has the maximum amplitude. Representative states A, B, C on semicircle (Fig.1) are given by: (A) $|\Delta_0| = |\Delta_{-1}| = 0$ and $|\Delta_1|^2 = -\alpha/4\beta$; (B) $|\Delta_0| = |\Delta_1| = 0$ and $|\Delta_{-1}|^2 = -\alpha/4\beta$; (C) $|\Delta_0|^2 = -\alpha/8\beta$ and $|\Delta_1|^2 = |\Delta_{-1}|^2 = -\alpha/16\beta$.

We obtain *other* minimum energy solutions by considering special cases in Eq. 13. (i) $|\Delta_1| = 0 = |\Delta_{-1}|$ and

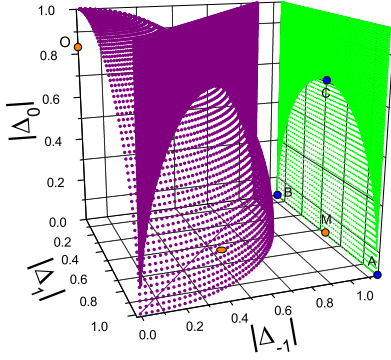


FIG. 1: (Color online) Geometric representation of p-wave states in population-imbalanced Fermi system. The semicircle formed by the intersection of sphere surface with plane represent a continuum of states exhibiting global energy minimum (see text). For clarity, plane containing semicircle is shown separately (green). O (on Δ_0 axis) and M (in Δ_1 - Δ_{-1} plane) are states with local energy minimum. Δ_m ($m = 0, \pm 1$)'s are normalized to the sphere radius $\sqrt{-\alpha/4\beta}$; $\alpha < 0$.

$|\Delta_0| \neq 0$: we find a unique solution, $|\Delta_0|^2 = -\alpha/6\beta$, shown as point O in Fig.1. (ii) $|\Delta_0| = 0$: this leads to equations for two ellipses in the $\Delta_1 - \Delta_{-1}$ plane:

$$\begin{aligned} |\Delta_1|^2 + 2|\Delta_{-1}|^2 + \frac{\alpha}{4\beta} &= 0 \quad (\text{ellipse1}) \\ 2|\Delta_1|^2 + |\Delta_{-1}|^2 + \frac{\alpha}{4\beta} &= 0 \quad (\text{ellipse2}) \end{aligned} \quad (16)$$

The intersection of the two ellipses gives the solution: $|\Delta_1|^2 = |\Delta_{-1}|^2 = -\alpha/12\beta$ and $|\Delta_0| = 0$; this is shown as point M in Fig.1. Like A and B, states O and M automatically satisfy phase constraint (Eq. 14(c)). We find these to exhaust all possible independent solutions. Incidentally, states A (B) respectively lie at the intersection of ellipse 1 (ellipse 2), and the sphere and plane of Fig.1. The ground state energies for states O and M are found to equal each other, and lie higher than the global minimum E_G^{gl} ; we denote this as *local* minimum energy:

$$E_G^{loc} = -\frac{\alpha^2}{12\beta} + \gamma \quad (\alpha < 0) \quad (17)$$

We checked the stability of the states, by examining the stability matrix or Hessian, H: $(\partial^2 E_G / \partial \Delta_{m_i} \partial \Delta_{m_j})$. We find that $\det[\mathbf{H}] = 0$ for states A and B, and $\det[\mathbf{H}] > 0$ for states O and M. In the language of Catastrophe Theory²⁶, A, B can be identified as non-Morse "critical" points, and O, M as Morse "critical" points. This is based on Morse lemma for Morse critical points, and Thom's theorem and splitting lemma for non-Morse critical points. $\det[\mathbf{H}] = 0$ occurs when one or more of the eigenvalues of the stability Hessian matrix H is zero. In

this case, Thom's splitting lemma can be used to represent the stability matrix H in a block-diagonal form, wherein H is split into blocks with non-zero determinants.²⁶

As can be seen from the expression for γ , and the definition of μ and h , in the limit of zero polarization, $P \rightarrow 0$, the GS energy coefficient $\gamma \rightarrow 0$, while $\alpha < 0, \beta > 0$ remain finite, but with different numerical values. Accordingly, the expressions for E_G^{gl} and E_G^{loc} remain essentially the same for $P \rightarrow 0$, but attain numerical values different from that for $P \neq 0$. The states A and B (equivalent to A by symmetry) correspond to the finding of Ref.¹⁸ in $P = 0$ case.

IV. SELF-CONSISTENT SOLUTIONS OF COUPLED GAP AND NUMBER EQUATIONS

Next, we self-consistently solve the set of three coupled gap equations (Eq. (8), and the two number equations (Eq. (9)). This is done for fixed population imbalance $P = (n_\uparrow - n_\downarrow)/(n_\uparrow + n_\downarrow)$, and p-wave coupling parameter g . (g is related to the triplet scattering parameter: $g = 25k_F^3 a_t / 8\pi$ for a cutoff $k_0 = 10k_F$). These detailed solutions of the p-wave superfluid states confirm the results obtained using free energy considerations (Sec. III above), and also reveal additional interesting features. We obtain the gap amplitudes Δ_m , and the chemical potentials μ_σ for different P and $1/k_F^3 a_t$. Using these, we obtain values of the ground state energy E_g from Eq. (7), as well as those of the coefficients α, β, γ that determine E_g . The agreement between our self-consistent solutions and analytical results for the ground state energies is good. We note that fixed $(P, n = n_\uparrow + n_\downarrow)$ is equivalent to fixed (μ, h) used in analytic study above.

A. Phase Stability and Construction of Phase Diagram

To check for *stability* of the p-wave states obtained from the self-consistent solutions, we enforce that the stability matrix $(\partial^2 E_G / \partial \Delta_{m_i} \partial \Delta_{m_j})$ is positive definite; and that $\delta p / \delta h > 0$. Based on this, we construct a polarization (P) - coupling ($1/k_F^3 a_t$) *phase diagram* in BEC-BCS crossover regime (Fig.2). Instability in the stability matrix can just indicate instability to another phase, but not the nature of the phase. However, this is sufficient to map out the phase boundary, e.g. the critical polarization line P_c , where superfluid gap vanishes. Above P_c , the system is in the normal phase. Below P_c , the stability of phases SF1 and SF2 are carefully examined in turn in the coupling-polarization space; this allows us to map out the full phase diagram.

In Fig. 2, SF1 denotes the stable superfluid phase corresponding to the states on the 'semicircle' in Fig.1 that give GS *global* minimum, E_G^{gl} (Eq. 15), i.e. with relative phase $\theta = 2n\pi$ among the gap parameters. E_G^{gl} and

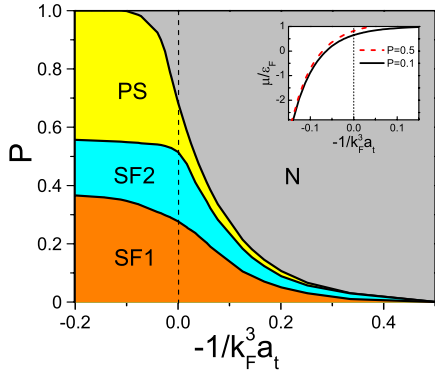


FIG. 2: (Color online) Polarization P vs p -wave coupling $-1/(k_F^3 a_t)$ phase diagram of two-component Fermi system with p -wave pairing. Shown are normal (N), p -wave superfluid phases (SF1; SF2), and phase separation (PS). Unitarity limit is shown by the dashed vertical line. Inset: Calculated chemical potential vs coupling across BCS and BEC regimes for $P = 0.1$ (solid line), 0.5 (dashed line). The Fermi energy, ϵ_F , is given by the line $\mu/\epsilon_F = 1$.

E_G^{loc} (Eq. 17) are given by the polarization-dependent parameters, α, β, γ . With increased polarization, α, β, γ (given by Eqs. 12 above), that determine E_G^{gl} and E_G^{loc} , change so that the superfluid phase SF2, corresponding to states with *local* minimum, attain energy lower than that of SF1, thereby becoming stable. This suggests the interesting possibility that at $T=0$, polarization may drive a quantum phase transition from SF1 to SF2. It may also be possible to access SF2 at $T \neq 0$. At even larger polarizations, for the same reason, SF2 becomes unstable to phase separation (PS). SF1, SF2, and PS occupy a relatively much narrower part of the phase diagram on the BCS side compared to the BEC side. In our two-component system with inter-species interaction, PS persists into full polarization, $P=1$. This is reasonable because at $P=1$, the system is essentially a one-component system in which the absence of minority species atoms makes inter-species interaction inoperative. Such a system can exhibit superfluidity only under the effect of intra-species interactions.

We note that since we have considered p -wave ($\ell = 1$) pairing with unlike spin components ($S = 1, m_s = 0$), the gap functions can be classified as $\ell = 1$ representations of the $O(3)$ group embedded in $O(6)$. Eq. (13) above reflects this $O(3)$ symmetry. Accordingly, the states in SF1, in particular the $\Delta_{1,\pm 1}$ states A and B, can be identified with the known "axial" or "ferromagnetic" phase, while the states in SF2, such O and M, with the known "polar" phase.

The inset in Fig. 2 shows the calculated behavior of chemical potential μ across the BEC-BCS regime. It deviates significantly from the Fermi energy (given by $\mu/\epsilon_F = 1$ line) in a wider region around the BEC-BCS crossover, even on the BCS side, and drops much more

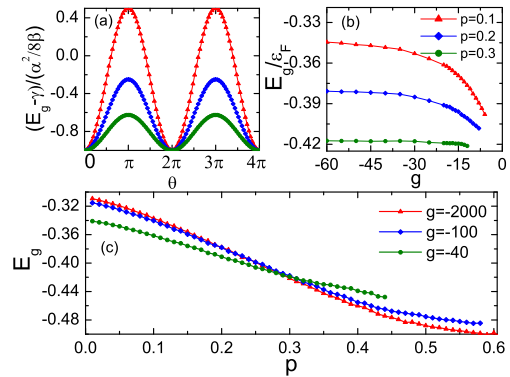


FIG. 3: (Color online) (a) Calculated ground state energy (scaled to global minimum) vs. relative phase angle θ (see text). Curve with maximal amplitude corresponds to the state C in Fig 1: $|\Delta_0|^2 = -\alpha/8\beta$, $|\Delta_1|^2 = |\Delta_{-1}|^2 = -\alpha/16\beta$. Other two curves respectively correspond to other representative states on the arc in Fig. 1: $|\Delta_0|^2 = -\alpha/11.3\beta$, $|\Delta_1|^2 = -\alpha/76.3\beta$, $|\Delta_{-1}|^2 = -\alpha/6.73\beta$, and $|\Delta_0|^2 = -\alpha/16\beta$, $|\Delta_1|^2 = -\alpha/186\beta$, $|\Delta_{-1}|^2 = -\alpha/5.49\beta$. (b) Calculated ground state energy E_g vs. coupling g for different polarizations P . (c) Calculated E_g vs. P for different g .

rapidly to negative values on the BEC side compared to the s -wave case. For sufficiently weak coupling in the BCS regime, μ approaches Fermi energy ϵ_F .

B. Variation of Ground state energy with Phase angle, Coupling and Polarization

Except for A, B, the continuum of "mixed" SF states on the semicircle (Fig.1) are characterized by a relative phase $2n\pi \leq \theta \leq (2n+2)\pi$, so that the energies of these states are expected to oscillate with θ . Results for three representative cases, obtained from our numerical calculations, are shown in Fig 3(a). For $\theta \neq 2n\pi$, the energies lie higher than the GS global minimum; the maximum amplitude occurring for the state C in Fig.1. This raises the possibility of observing θ -oscillation in each of the states on the semicircle using phase sensitive experimental technique(s). They could also be accessed at finite- T .

Figs. 3b, 3c respectively show the variation of E_g with coupling g at fixed polarizations P , and with P for fixed g . E_g is normalized to the Fermi energy $\epsilon_F = \hbar^2 k_F^2 / 2m$, with $2k_F^3 = k_{F\uparrow}^3 + k_{F\downarrow}^3$. For a given P , E_g becomes less negative as g approaches unitarity; the trend is more noticeable for smaller P 's. The energy curves in Fig. 3(b) would terminate at some non-zero coupling, and hence not expected to cross. Extrapolated to normal regime, energies corresponding to different polarizations would be different, and also not cross. For a given g , E_g lies higher for smaller P , presumably due to the lower majority-species band becoming progressively more occupied with increasing P , thereby lowering E_g with increasing P .

larization. For small P , E_g becomes less negative with increasing g . This trend is reversed for $P \geq 0.3$. The crossing at $P \approx 0.3$ is suggestive of a possible scaling using stretches in P and E_g .

V. SUMMARY

We have presented several new results for p-wave pairing in two-component population imbalanced Fermi systems for the case when inter-species pairing interaction is dominant, across the entire BCS-BEC regimes. The ground state structure as a function of population imbalance is rich, involving various sub-states of orbital angular momentum $\ell = 1$. We find states giving both global and local energy minimum that we associate with non-Morse and Morse critical points. The 3D geometric rendering of our analytic solutions of the SF states provides added insight into these. Our detailed numerical calculations suggest a possible quantum phase transition between two superfluid phases driven by polarization. The energies of a multitude of "mixed" SF states show oscillations with a relative phase angle, that may be observed in phase sensitive experiments. Insight into the nature

of the orbital part of our superfluid states may be gained from measuring the angular dependence of momentum distributions; from molecular spectroscopy using light radiation; or possibly measurements of zero sound attenuation. While this work has not considered possibilities such as the FFLO states with non-zero center-of-mass momentum (mentioned in Sec. II), or "breached pair" states²⁷, our findings suggest that the problem of $q = 0$ unconventional pairing for population imbalanced systems, even at the mean-field level, is interesting in itself. Additionally, this work may form a basis for exploring the possibility of non-s-wave "breached pair" superfluidity in BCS or BEC region. Our work should be of interest to other unequal population Fermi systems, especially where p-wave intra-species couplings are small or negligible.

VI. ACKNOWLEDGEMENTS

We acknowledge helpful discussions with Jason Ellis, Randy Hulet, Harry Kojima, and Adriana Moreo. The work was partly supported by funding from ICAM. One of us (F. Popescu) acknowledges an ICAM Fellowship.

-
- ¹ Y. Maeno, H. Hashimoto, K. Yoshida, S. Nishizaki, T. Fujita, J.G. Bednorz, and F. Lichtenberg, *Nature* **372**, 532 (1994).
- ² S. S. Saxena, P. Agarwal, K. Ahilan, F. M. Grosche, R. K. W. Haselwimmer, M. J. Steiner, E. Pugh, I. R. Walker, S. R. Julian, P. Monthoux, G. G. Lonzarich, A. Huxley, I. Sheikin, D. Braithwaite, and J. Flouquet, *Nature (London)* **406**, 587-592 (2000); C. Pfeiderer, M. Uhlarz, S. M. Hayden, R. Vollmer, H. v. Lohneysen, N. R. Bernhoeft, and G. Lonzarich, *Nature* **412**, 59 (2001); Dai Aoki, Andrew Huxley, Eric Ressouche, Daniel Braithwaite, Jacques Flouquet, Jean-Pascal Brison, Elsa Lhotel, and Carley Paulsen, *Nature (London)* **413**, 613 (2001); N. T. Huy, A. Gasparini, D. E. de Nijs, Y. Huang, J. C. P. Klaasse, T. Gortenmulder, A. de Visser, A. Hamann, T. Gorklach, and H. v. Lohneysen, *Phys. Rev. Lett.* **99**, 067006 (2007).
- ³ R. Casalbuoni and G. Nardulli, *Rev. Mod. Phys.* **76**, 263 (2004).
- ⁴ W. A. Coniglio, L. E. Winter, K. Cho, C. C. Agosta, B. Fravel, and L.K. Montgomery, *Phys. Rev. B* **83**, 224507 (2011).
- ⁵ M. W. Zwierlein, A. Schirotzek, C. H. Schunck, W. Ketterle, *Science* **311**, 492 (2006); G. B. Partridge, W. Li, R. I. Kamar, Y.-an Liao, R. G. Hulet, *Science* **311**, 503 (2006); M. W. Zwierlein, C. H. Schunck, A. Schirotzek, and W. Ketterle, *Nature (London)* **442**, 54 (2006); Y. Shin, M. W. Zwierlein, C. H. Schunck, A. Schirotzek, and W. Ketterle, *Phys. Rev. Lett.* **97**, 030401 (2006); G. B. Partridge, Wenhui Li, Y. A. Liao, and R. G. Hulet, *Phys. Rev. Lett.* **97**, 190407 (2006); Y. Shin, C. H. Schunck, A. Schirotzek, and W. Ketterle, *Nature* **451**, 689 (2008).
- ⁶ C.A. Regal, M. Greiner, D. S. Jin, *Phys. Rev. Lett.* **92**, 040403 (2004); M. W. Zwierlein, C. A. Stan, C. H. Schunck, S. M. F. Raupach, A. J. Kerman, and W. Ketterle, *Phys. Rev. Lett.* **92**, 120403 (2004); C. Chin, M. Bartenstein, A. Altmeyer, S. Riedl, S. Jochim, J. Hecker Denschlag, and R. Grimm, *Science* **305**, 1128 (2004).
- ⁷ J. Zhang, E.G.M. van Kempen, T. Bourdel, K. Khaykovich, J. Cubizolles, F. Chevy, M. Teichmann, L. Tarruell, S.J.J.M. F. Kokkelmans, and C. Salomon, *Phys. Rev. A* **70**, 030702(R) (2004).
- ⁸ C.A. Regal, C. Ticknor, J.L. Bohn, and D.S. Jin, *Phys. Rev. Lett.* **90**, 053201 (2003).
- ⁹ C. Ticknor, C.A. Regal, D.S. Jin, and J.L. Bohn, *Phys. Rev. A* **69**, 042712 (2004).
- ¹⁰ C.H. Schunck, M.W. Zwierlein, C.A. Stan, S.M.F. Raupach, W. Ketterle, A. Simoni, E. Tiesinga, C.J. Williams, and S. Julienne, *Phys. Rev. A* **71**, 045601 (2005).
- ¹¹ Y. Nishida, arXiv:0810.1321 (2009)
- ¹² Y.-J. Han, Y.-H. Chan, W. Yi, A. J. Daley, S. Diehl, P. Zoller, and L.-M. Duan, *Phys. Rev. Lett.* **103**, 070404 (2009).
- ¹³ C. Lai, C. Shi, S. -W. Tsai, arXiv:1206.6797 (2012).
- ¹⁴ V. Gurarie, L. Radzihovsky, A.V. Andreev, *Phys. Rev. Lett.* **94**, 230403 (2005).
- ¹⁵ C.-H. Cheng and S.-K. Yip, *Phys. Rev. Lett.* **95**, 070404 (2005).
- ¹⁶ S. S. Botelho, C.A.R. Sá de Melo, *J. Low Temp. Phys.* **140**, 409 (2005); M. Iskin and C.A.R. Sá de Melo, *Phys. Rev. Lett.* **96**, 040402 (2006).
- ¹⁷ Y. Ohashi, *Phys. Rev. Lett.* **94**, 050403 (2005).
- ¹⁸ Tin-Lun Ho and Roberto B. Diener, *Phys. Rev. Lett.* **94**, 090402 (2005).
- ¹⁹ A. Bulgac, M. Forbes, and A. Schwenk, *Phys. Rev. Lett.* **97**, 020402 (2006); Kelly R. Patton and D. E. Sheehy, *Phys. Rev. A* **83** 051607 (2011).

- ²⁰ P. Fulde, and R. A. Ferrell, Phys. Rev. **135** A550 (1964); A. I. Larkin and Yu.N. Ovchinnikov, Zh. Eksp. Teor. Fiz. **47** 1136 (1964).; A. I. Larkin and Yu.N. Ovchinnikov, Sov. Phys. JETP **20** 762 (1965);
- ²¹ Standard definitions, $G_{\sigma,\sigma'} \equiv -\langle T_{\tau} c_{\mathbf{k}\sigma}(\tau) c_{\mathbf{k}\sigma'}^{\dagger}(0) \rangle$, and $F_{\sigma,\sigma'} \equiv -\langle T_{\tau} c_{-\mathbf{k}\sigma'}^{\dagger}(\tau) c_{\mathbf{k}\sigma}^{\dagger}(0) \rangle$ are used; see Ref²².
- ²² H. Bruus and K. Flensberg, *Introduction to Many-body Quantum Theory in Condensed Matter Physics* (Oxford University Press Inc. New York, 2004).
- ²³ R. Liao and K. Quader, Phys. Rev. B **76**, 212502 (2007).
- ²⁴ P. Nozières and S. Schmitt-Rink, J. of Low Temp. Phys. **59**, 195 (1985).
- ²⁵ This allows g to be expressed in terms of scattering parameters, viz. triplet scattering volume a_t and an effective range or equivalently a cut-off momentum k_0 ; see, for example, M. Iskin and C.A.R. Sá de Melo, Phys. Rev. A **74**, 013608 (2006).
- ²⁶ R. Gilmore, *Catastrophe Theory for Scientists and Engineers* (Dover Publications Inc., New York, 1993).
- ²⁷ W. V. Liu and F. Wilczek, Phys. Rev. Lett. **90**, 047002 (2003); M.M. Forbes, E. Gubankova, W.V. Liu, and F. Wilczek, Phys. Rev. Lett. **94**, 017001 (2005).